*Reprinted from the April 1975*
*Journal of Lubrication Technology*

**P. K. Gupta**
Mechanical Technology Inc.,
Latham, N. Y.

# Transient Ball Motion and Skid in Ball Bearings

*The generalized differential equations of motion of the ball in an angular contact ball bearing operating under elastohydrodynamic traction conditions are formulated and integrated with prescribed initial conditions. A complete transient and steady state motion is thus obtained to predict the amount of skid and resulting wear rates for a set of given operating conditions. The analysis provides an up-to-date design tool in predicting skid and ball motion as a whole in ball bearings operating under arbitrary ball-race traction characteristics.*

## Introduction

With increasing numbers of high speed ball bearing applications, the interest in analyzing the true dynamic behavior of the bearing elements has been continuously growing. Most of the kinematic treatments of ball bearings until recently have been limited to the hypotheses of inner or outer race control postulated by Jones [12,13] and, thus, the ball angular velocity vector is clearly defined and a quasi-static force balance type of calculation is carried out to estimate the bearing behavior. Based on such simplified hypotheses, Poplawski and Mauriello [15] have presented a simple analysis for predicting skidding in angular contact ball bearings.

Harris [7] has recently proposed that race control is generally valid for high speed bearings when the traction coefficient at the ball race contacts is high enough to prevent any gyroscopic slip. Also, in his later work [8] it has been pointed out that these simple kinematic hypotheses do not hold under elastohydrodynamic conditions. With a very simple elastohydrodynamic traction model, Harris [8] has modified the existing force balance type of analysis to avoid the use of race control theories. The convergence of the solution of the nonlinear equations is such that a modified quasi-static analysis will strongly depend on the traction-slip characteristics. Furthermore, in applications where the balls are continuously accelerating and decelerating a force balance type of computation may be quite meaningless.

A dynamic formulation of motion of the various bearing elements has been presented by Walters [18]. This work is basically concerned with the dynamics of the separator and a constrained ball motion is assumed. Nevertheless, the resulting differential equations of motion are integrated to obtain the true motion. The constraints on the ball motion require that the contact angles and loads as a function of the orbital position of the ball are predetermined by a simple conventional quasi-static analysis where the effects of centrifugal forces have been included. Thus, the contact angles and loads are not influenced by any dynamics of the bearing elements. Since the dynamic variations in applied loads and the dynamic changes in race angular velocity, resulting in variations in centrifugal force, will result in dynamic variations in the contact angles, it is clear that the constrained ball motion assumption will not hold under such dynamic conditions. Hence, the formulation cannot be used for investigating skid and other transient phenomenon in ball bearings. Furthermore, in a lubricated bearing validity of a constrained motion, established by quasi-static methods of Jones [12, 13], where no gyroscopic slip is allowed, is still questionable and a generalized solution of the ball motion in a six degree of freedom system is necessary in order to provide any support to such a holonomic system.

Significant advancements have been made in understanding the lubrication mechanics at ball race contacts. The classical Dawson Higginson's Theory [4] for computing lubricant film thickness in cylinderical elastohydrodynamic (EHD) contacts has been modified by Cheng [2, 3] to include the thermal effects and side leakage in elliptical contacts. A substantial experimental work has also been reported in this area as compiled by McGrew et al. [14]. Based on the available formulation for elastohydrodynamic theory Smith et al. [16] have correlated experimental traction-slip data with a semi-empirical lubrication model for polyphenyl ether. Similar work with 7808 MIL oil has also been reported [17]. On the basis of experimental data obtained by Johnson and Cameron [11], Gu [6] has presented a lubrication model relevant to most mineral oils and it is shown that the model agrees extremely well with the experimental observations of Allen, et al. [1].

[1] Numbers in brackets designate references at end of paper.

Contributed by the Lubrication Division of THE AMERICAN SOCIETY OF MECHANICAL ENGINEERS and presented at the ASME-ASLE-Joint Lubrication Conference, Montreal, Canada, October 8-10, 1974. Manuscript received by the Lubrication Division, May 20, 1974. Paper No. 74-Lub-9.

The primary objective of this paper is to formulate the generalized differential equations of motion for a ball in a thrust loaded angular contact bearing. The motion is considered with the six degrees of freedom and it is shown that these equations may be integrated with arbitrary traction-slip relation and any set of initial conditions. Two different EHD ball-race traction models available in the literature [6, 16] are used in the formulation. Transient ball motion under such realistic traction models is studied when the inner race is accelerated and hence a dynamic simulation of skid in a lubricated bearing is obtained. The differential equations are properly nondimensionalized and a conventional Fourth Order Runga-Kutta-Merson method [5] is used to numerically integrate the system and check the truncation errors of each time step to ensure convergence. Also, steady state solutions under the different ball-race traction models compared with those obtained by the conventional force balance type of methods due to Jones [12, 13].

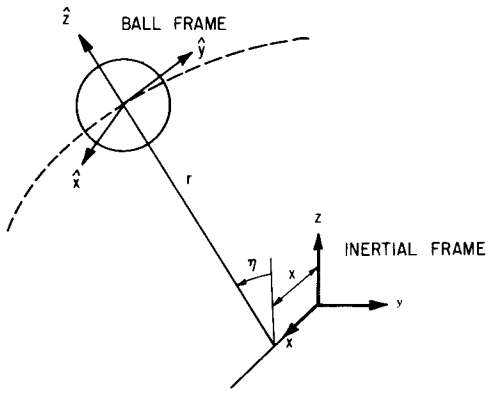

Fig. 1 Ball coordinate frames

## Equations of Ball Motion

The complete motion of the ball is obtained by considering the translational and orbital motion of the center of the mass in the cylindrical inertial coordinate frame $(x, r, \eta)$ and the rotational motion of the ball about its mass center in the ball frame $(\hat{x}, \hat{y}, \hat{z})$ as shown in Fig. 1. Generally the $(\hat{x}, \hat{y}, \hat{z})$ system is fixed in the body along the principal inertial axes, but if the balls are perfectly spherical any orthogonal system is equally convenient to describe the motion. Hence, $\hat{x}, \hat{y}, \hat{z}$ is selected such that the $\hat{z}$ axis lies along the radius vector **r** and the $\hat{x}$ axis is parallel to the inertial axis $x$. Denoting the mass of the ball by m and the moment of inertia by I, the equations of motion are described as:

$$\begin{aligned} m\ddot{x} &= F_x \\ m(\ddot{r} - r\dot{\eta}^2) &= F_r \\ m(r\ddot{\eta} + 2\dot{r}\dot{\eta}) &= F_\eta \end{aligned} \tag{1}$$

$$\begin{aligned} I\dot{\omega}_{\hat{x}} &= G_{\hat{x}} \\ I\dot{\omega}_{\hat{y}} - I\omega_{\hat{z}}\dot{\eta} &= G_{\hat{y}} \\ I\dot{\omega}_{\hat{z}} + I\omega_{\hat{y}}\dot{\eta} &= G_{\hat{z}} \end{aligned} \tag{2}$$

where $F_x$, $F_r$, $F_\eta$ denote the components of the applied force vector, **F**. $G_x$, $G_y$, $G_z$ represent the components of applied moment vector **G** and the ball angular velocity is denoted by the components $\omega_x$, $\omega_y$, $\omega_z$. Also, the first derivatives are denoted by a dot ("·") over the variable and the second derivative is represented by two dots. The orbital velocity of the ball is clearly $\dot{\eta}$.

It should be noted that the contact forces at ball race contact, and resulting tractive forces (with a prescribed traction-slip relation) form the applied force and moment vectors **F** and **G**.

## Applied Force and Moment Vectors

The vectors **F** and **G** in equations (1) and (2) denoting the applied forces and moments are to be determined at any position of the ball relative to the races. The races will be allowed to accelerate only about their axes and the relative position will be determined by satisfying the static equilibrium. Therefore, let the position of the inner race and the balls be specified relative to the outer race. In order to determine the total forces and moments on the ball, the elastic contact forces and the resulting tractive forces, which will generally be a function of local slip velocity, are to be determined. Thus, solution of race equilibrium equations and the kinematics of the ball will be required at any prescribed position of the ball relative to the outer race. When only a thrust load is applied axially, the position of the inner race is determined by satisfying the equilibrium equation along the bearing axis.

**1 Race Equilibrium.** Let the position of a ball be denoted by $(x, r)$ in the inertial frame $(x, r, \eta)$ as shown in Fig. 2. The origin of the inertial frame is selected so that the centers of curvature of outer race lie on a circle which has the center at the origin, lies in a plane normal to the $x$ axis and has a radius, $r_1$. Also, let $r_e$ denote the radius of the pitch circle, which is defined such that if $r = r_e$, the contact force is zero. Thus, under no load conditions

$$(f_1 - 0.5)d \cos \alpha^0 = r_e - r_1 \tag{3}$$

## Nomenclature

$a$ = length of semimajor axis of contact ellipse (in)
$A$ = dimensionless semimajor axis
$b$ = length of semiminor axis of contact ellipse (in)
$B$ = dimensionless semiminor axis
$d$ = ball diameter (in)
$D$ = dimensionless ball diameter
$E$ = Young's modulus of elasticity (lb/in$^2$)
**F** = applied force vector, (lb)
**F*** = dimensionless applied force vector
**G** = applied moment vector (in-lb)
**G*** = dimensionless moment vector
$I$ = ball moment of inertia (lb-in-sec$^2$)
$K$ = wear coefficient
$K_f$ = thermal conductivity of lubricant (lb/sec °F)
$m$ = mass of the ball (lb-sec/in$^2$)
$Q$ = ball race contact load (lb)
$Q^0$ = static ball-race contact load (lb)
$Q_t$ = applied thrust load
$R$ = dimensionless radial position
$r_0$ = characteristic length (in)
$S$ = dimensionless position of inner race
$t$ = time (sec)
$T_0$ = inlet temperature (°R)
**u** = slip velocity vector (in/sec)
$V$ = sliding velocity (in/sec)
$W$ = wear rate (in$^3$/sec)
$\alpha$ = contact angle
$\beta$ = viscosity-temperature coefficient (°R)
$\beta_1$ = viscosity-temperature coefficient (1/°R)
$\delta$ = normal contact deflection
$\rho$ = curvature of elastically deformed surface (1/in)
$\kappa$ = traction coefficient
$\mu_0$ = inlet viscosity (lb-sec/in$^2$)
$\tau$ = dimensionless time

### Coordinate Frames

$(x,r,\eta)$ = inertial frame
$(\hat{x},\hat{y},z)$ = ball frame
$(x,y,z)$ = coordinate frame along the contact load
$(\xi,\zeta)$ = axes in the contact ellipse

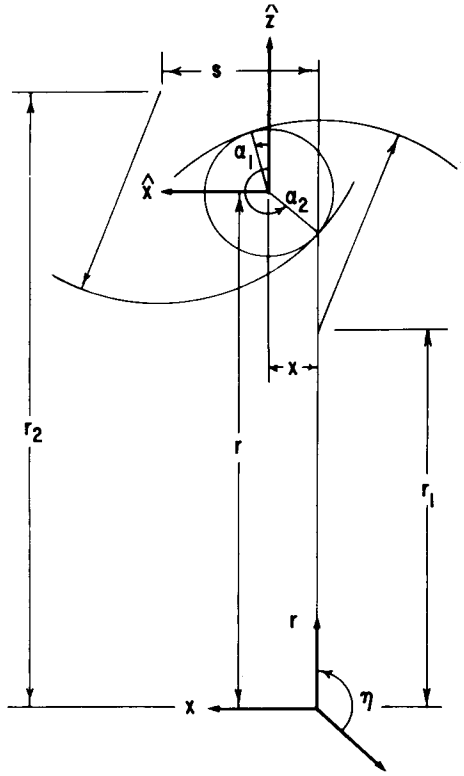


Fig. 2 Coordinate frames defining the relative positions of ball and the races

where $d$ is the ball diameter, $\alpha^0$ is the free contact angle, and $f_1$ is the outer race curvature factor.

Let the ball position and outer race curvature center be measured relative to its no load position and $r_0$ be a characteristic length which scales all linear dimensions. Thus,

$$D = \frac{d}{r_0};\ R_e = r_e/r_0;\ R_1 = (r_e - r_1)r_0;\ R = (r - r_e)/r_0;\ X = x/r_0 \qquad (4)$$

The contact angle $\alpha_1$ and the contact deflection $\delta_1$ and load $Q_1$ are given by

$$\sin \alpha_1 = \frac{X}{\sqrt{X^2 + (R + R_1)^2}}$$

$$\bar{\delta}_1 = \frac{\delta_1}{r_0} = \sqrt{X^2 + (R + R_1)^2} - (f - 0.5)D \qquad (5)$$

$$Q_1 = \frac{4\sqrt{2}\,E' r_0^2}{3\sqrt{\Sigma\rho_1^*}} \left(\frac{\bar{\delta}_1}{\delta_1^*}\right)^{3/2}$$

where $E'$, $\Sigma\rho_1^*$, and $\delta_1$ are described in the Appendix. Also the size of the contact ellipse may be determined by the formulae summarized in Appendix.

The axial position of the inner race will in general be determined by the dynamic equation of motion of the race. This clearly will also involve the dynamics of the remainder of the system of which the bearing is a part. In order to avoid such system complications the present investigation is restricted to static equilibrium of the inner race. Also, it may be noted that the component of the ball race tractive force along the bearing axis will generally be small compared to the absolute value to the tractive force vector since the gyroscopic slip will be small compared to the slip in the rolling direction. Furthermore, since the absolute tractive force itself is small compared to the applied load it is justifiable to exclude the tractive force component from the static equilibrium equation of the race in the axial direction.

Similar to the outer race, let the inner race curvature centers lie on the circle of radius $r_2$ in a plane normal to the $x$ axis and a distance $s$ from the origin as shown in Fig. 2. Also, define the nondimensional quantities

$$S = s/r_0;\ R_2 = (r_2 - r_e)/r_0. \qquad (6)$$

Again under no load condition the contact angle is $\alpha^0$ and the inner race position is determined by geometry

$$\cos \alpha^0 = \frac{R_2 - R}{(f_2 - 0.5)D}$$

$$S = X + \sqrt{\{(f_2 - 0.5)D\}^2 + (R_2 - R)^2} \qquad (7)$$

where $f_2$ is the inner race curvature factor.

If the contact angle under load is $\alpha_2$, as shown in Fig. 2, the normal contact deflection and load are given by

$$\bar{\delta}_2 = \frac{\delta_2}{r_0} = \frac{R - R_2}{\cos \alpha_2} - (f_2 - 0.5)D$$

and (8)

$$Q_2 = \frac{4\sqrt{2}\,E' r_0^2}{3\sqrt{\Sigma\rho_2^*}} \left(\frac{\bar{\delta}_2}{\delta_2^*}\right)^{3/2}$$

Denoting the applied thrust load by $Q_a$, the static equilibrium equation along the bearing axis is written as

$$Q_2 \sin \alpha_2 + Q_t = 0 \qquad (9)$$

$Q_2$ may be eliminated from equations (8) and (9) and the resulting nonlinear equation in $\alpha_2$ is solved by Newton-Raphson iteration method. Once $\alpha_2$ is known, the computation of contact load $Q_2$ is straight forward from equation (8). The axial position of the inner race, $S$, is determined by geometry.

$$S = X + (R_2 - R) \tan \alpha_2 \qquad (10)$$

**2 Ball-Race Slip and Tractive Forces.** In order to determine

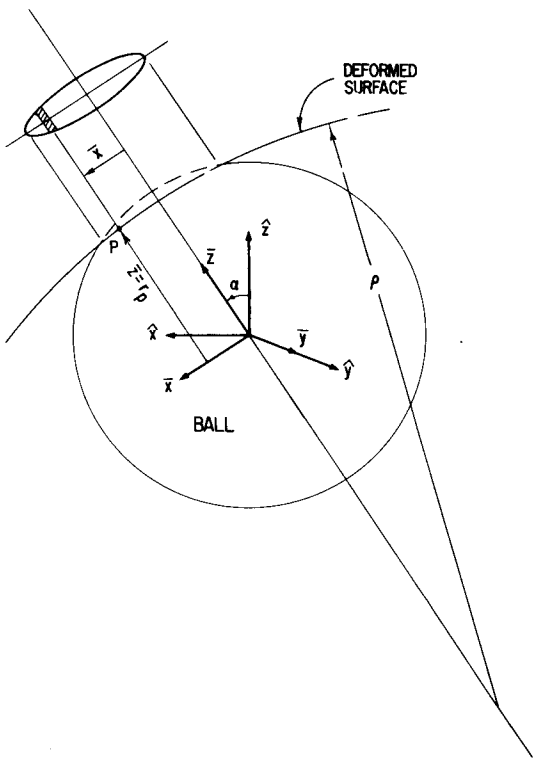


Fig. 3 Contact ellipse axes relative to ball reference frames

the tractive forces at the ball-race contacts the local slip velocity vector at any point must be determined for any point within the contact ellipse.

Consider the coordinate frame $(x, y, z)$ as shown in Fig. 3. The position vector of any point $P$ in this frame is given by

$$\mathbf{R}_p = \begin{Bmatrix} \bar{X}A \\ 0 \\ \sqrt{\rho^2 - (XA)^2} - \sqrt{\rho^2 - A^2} + \sqrt{\frac{D^2}{4} - A^2} \end{Bmatrix} \tag{11}$$

where $\rho$ is the radius of curvature of the deformed surface as is given by

$$\rho_i = \frac{2f_i D}{2f_i + 1}$$

where $f_i$ is the race curvature factor for outer and inner races corresponding to $i = 1$ and $i = 2$, respectively. Also $\bar{X}_i = \bar{x}/a_i$, $A_i = a_i/r_0$. $\mathbf{R}_p = \mathbf{r}_p/r_0$.

If the ball angular velocity vector is $\hat{\omega}$ in the $(\hat{x}, \hat{y}, \hat{z})$ system, the translational velocities are given by $\dot{X}$, $\dot{R}$, and the orbital speed is $\dot{\eta}$ in the inertial frame, then the ball velocity at point $P$ in the $(\bar{x}, \bar{y}, \bar{z})$ system is given by

$$\mathbf{v}_b = [T(\alpha)]\hat{\omega} \times \hat{\mathbf{R}}_p + [T(\alpha)]\begin{Bmatrix} \dot{X} \\ -\eta(R + R_e) \\ \dot{R} \end{Bmatrix} \tag{12}$$

where the transformation matrix $T(\alpha)$ is given by

$$[T(\alpha)] = \begin{bmatrix} \cos\alpha & 0 & -\sin\alpha \\ 0 & 1 & 0 \\ \sin\alpha & 0 & \cos\alpha \end{bmatrix}$$

The race angular velocity $\omega_r$ will have only one component along the $x$ axis, but for brevity the vector notation will be preserved. Race velocity at point $P$ in the $(\bar{x}, \bar{y}, \bar{z})$ system is thus given by

$$\mathbf{v}_r = [T(\alpha)]\left\{\omega_r \times \left\{\mathbf{R}_p + [T(\alpha)]\begin{Bmatrix} X \\ 0 \\ R + R_e \end{Bmatrix}\right\}\right\} \tag{13}$$

The local slip velocity is obtained by subtracting (12) and (13).

$$\mathbf{u} = \mathbf{v}_r - \mathbf{v}_b \tag{14}$$

If the length of semiminor axis, $b$ is small compared to that of the semimajor axis, $a$, then the slip variations along the minor axis may be neglected. For most bearing geometries, the ratio $a/b$ is indeed large and, hence, such an approximation is relevant.

The tractive force in the contact ellipse will have two components in a general case with gyroscopic slip along the $\xi$ axis and tractive slip along the $\zeta$ direction (see Fig. 4). If a traction coefficient is defined as a vector $\kappa$ having components $\kappa_1$ and $\kappa_2$ along the $\xi$ and $\zeta$ axes, then the tractive force vector is defined to have the components

$$dF_1 = \kappa_1(\mathbf{u})dQ \quad \text{and} \quad dF_2 = \kappa_2(\mathbf{u})dQ \tag{15}$$

where $dQ$ is the normal contact load over any elementary area in the contact ellipse. Since the variations of slip in the $\zeta$ direction is neglected, an elementary area is defined as shown in Fig. 4. Now $dF_1$, $dF_2$, and $dQ$ are quantities per unit length along the $\xi$ axis. Normal load is defined by the Hertzian pressure distribution, thus

$$\frac{dQ}{d\bar{\xi}} = \frac{\pi}{2} p_H ab(1 - \bar{\xi}^2) \tag{16}$$

where

$$\bar{\xi} = \xi/a.$$

Combining equations (15) and (16) the net force vector per unit length along the $\xi$ axis and the resulting tractive moment are given by

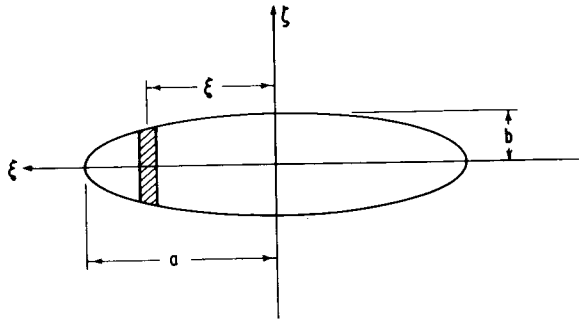


Fig. 4 Contact ellipse

$$d\mathbf{F}' = \frac{\pi}{2} p_H ab(1 - \bar{\xi}^2)\begin{Bmatrix} \kappa_2[\mathbf{u}(\bar{\xi})] \\ \kappa_2[\mathbf{u}(\bar{\xi})] \\ -1 \end{Bmatrix} d\bar{\xi}$$
$$d\mathbf{G} = \mathbf{R}_p \times d\mathbf{F}' \tag{17}$$

Since, in the equations of motion, the moments are required in the $(\hat{x}, \hat{y}, \hat{z})$ system and the force is to be transformed in the $(x, \eta, r)$ frame equation (17) must be properly transformed. Also by definition of $(\hat{x}, \hat{y}, \hat{z})$ frame it is clear that the components along the three orthogonal axes of both frames will be equal. Thus,

$$\mathbf{F} = [T(\alpha)]\int_{-1}^{1} d\mathbf{F}'$$
$$\mathbf{G} = [T(\alpha)]\int_{-1}^{1} d\mathbf{G}' \tag{18}$$

The integrals shown in equations (18) are obtained numerically using the conventional Gaussian Quadrature methods when the traction slip relation $\kappa$ [u $(\xi)$] is prescribed. This relationship is generally derived from the lubrication model at the ball-race contact.

**3 Lubrication Models.** A realistic lubrication model for the ball-race contact is indeed a dominating factor in determining the dynamic response of a bearing. With all the experimental data available for various lubricants and several versions of the EHD analyses, the two semi-empirical models presented in the literature may be used for establishing the tractionslip relationship under EHD conditions. Just for comparison purposes a constant traction coefficient is also considered as a possible model.

**Model I.** Based on the theoretical foundation for elastohydrodynamic theory [2, 3, 4] and available experimental data [11], Gu [6] has postulated a semiempirical model for predicting traction as a function of slip. It is shown that the traction coefficient $\kappa_2$ in the rolling direction is dependent on three parameters.

$$G_1 = \frac{\mu_0 u_2}{p_H h}; \quad G_2 = \frac{\beta_1 \mu_0 u_2^2}{8K_f}; \quad G_3 = \gamma p_H \tag{19}$$

where $\mu_0$ is the lubricant viscosity (lb-sec/in$^2$) at an inlet temperature of $T_0$ ($^\circ R$). $K_f$ is the thermal conductivity (lb/sec°F) of the lubricant $h$ is the film thickness (in), $u_2$ is the slip velocity (in/sec) in the rolling direction, $p_H$ is the maximum Hertz pressure and the coefficients $\gamma$ and $\beta_1$ are obtained from the viscosity-pressure-temperature model of the form

$$\mu(p,T) = \mu_0 \exp\,[\gamma_p - \beta_1(T - T_0)] \tag{20}$$

The relationship between $G_1$, $G_2$, $G_3$ and the traction coefficient $\kappa_2$ is represented graphically [14] by a series of graphs and this data is basically stored in a computer data file for real applications. The film thickness $h$ is computed by the methods of Dawson-Higginson [4] and Cheng [2, 3].

With the assumptions of a narrow contact ellipse this model is directly applicable to a ball-race contact. In equation (19) $p_H$ is

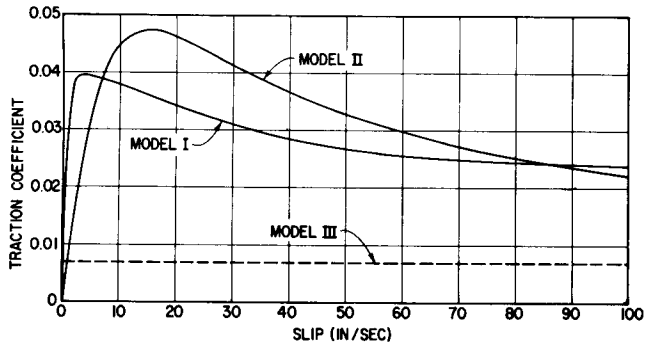


Fig. 5 Traction slip relations at the inner race contact obtained with the various traction models. Rolling speed = 1500 in/sec; Maximum Hertz pressure = 95000 psi; Semimajor axis = 0.028 in and semiminor axis = 0.0032 in

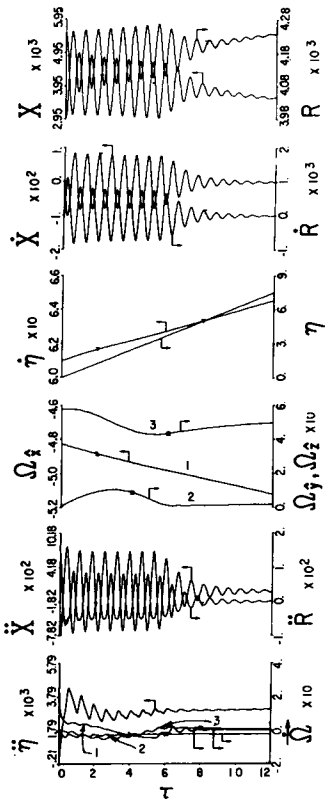

Fig. 6 Ball motion solutions in dimensionless form

replaced by the pressure as a function of $\xi$

$$p_\xi = p_H \sqrt{1 - \left(\frac{\xi}{a}\right)^2}$$

and $u_2$ is clearly a function of $\xi$ as determined by equation (14). Thus $\kappa_2$ is obtained as a function of $\xi$. In the case of gyroscopic slip, there will be a slip component $u_1$, which is a direction perpendicular to rolling. If this velocity is small compared with the slip in the rolling direction, then it is shown that the traction coefficient normal to the rolling direction is expressed as

$$\kappa_1 = \kappa_2 \frac{u_1}{u_2} \tag{21}$$

This model agreed extremely well with the experimental torque data obtained by Allen, et al. [1]. The required lubricant data for the present investigation is assumed to be same as that used in references [1] and [6], $\gamma = 9.2 \times 10^{-5}$ in$^2$/lb, $\beta_1 = 0.028$/deg F, $K_f = 0.0216$ lb/sec deg F, $\mu_0 = 6 \times 10^{-5}$ lb-sec/in$^2$ and the inlet temperature, $T_0 = 83$ deg F. Note that the temperature-viscosity coefficient, $\beta$, in computations of thermal reduction factors due to Cheng [2] is defined by the relation

$$\mu_0 = \mu_0 \exp\left[\gamma_p + \beta\frac{1}{T} - \frac{1}{T_0}\right]$$

A value for this coefficient is extracted by comparing the above relation with equation (20). $\beta = 8301$ °R found to be consistent.

**Model II.** Other than the above model, Smith et al. [16] have proposed a traction model based on the experimental data obtained by them for polyphenyl ether. It is shown that the shear stress in the lubricant is best correlated by an expression

$$\sigma_{\xi\zeta} = \frac{\mu_0 u_2 \sin^{-1}[\psi \exp(\gamma^* p/2)] \exp(\gamma^* p/2)}{h\psi\sqrt{1 + \psi^2 \exp(\gamma^* P)}}$$

where (22)

$$\psi = u_2 \sqrt{\frac{\mu_0 \beta^*}{8K_f}}$$

$p$ is the local pressure obtained by Hertzian pressure distribution and other parameters are the same as defined earlier. The three empirical constants $\mu_0^*$, $\gamma^*$, $\beta^*$ are determined by correlating the experimental data.

Once again with the assumption of narrow ellipse equation (22) may be integrated with respect to $\zeta$ to obtain a tractive force per unit length along the major axis $\xi$. If this force is divided by the normal force per unit length a traction coefficient $\kappa_2$ is the rolling direction determined. Some straightforward algebraic manipulation will show that

$$\kappa_2(\xi) = \frac{4}{\pi} \frac{\mu_0 u_2}{h\psi^2 p_\xi} J(\xi)$$

where

$$J(\xi) = \int_0^1 \frac{\varphi(\xi,\zeta) \ln[\varphi(\xi,\zeta) + \sqrt{1 + \varphi^2(\xi,\zeta)}]}{\sqrt{1 + \varphi^2(\xi,\zeta)}} d\zeta \tag{23}$$

$$\varphi(\xi,\zeta) = \psi \exp[\gamma\sqrt{1 - \zeta^2}/2]$$

and

$$\zeta = \zeta/b_\xi$$

Traction coefficient in the $\xi$ direction, due to gyroscopic slip $u_1$ is again estimated by the approximation used by Gu [6]

$$\kappa_1(\xi) = \kappa_2(\xi)\frac{u_1}{u_2} \tag{24}$$

Since the model is shown to be valid for polyphenyl ether the lubricant data used for the computation of film thickness and thermal reduction factors is extracted from reference [16]. The required data are $\mu_0 = 2.5639 \times 10^{-6}$ lb-sec/in$^2$, $\gamma = 9.8623 \times 10^{-5}$ in$^2$/lb, $\beta = 6.5042 \times 10^3$ °R, $T_0 = 670$ °R, $K_f = 0.01205$ lb/sec deg F. The empirical constants $\mu_0^*$, $\gamma^*$, and $\beta^*$ are shown to be quite insensitive to rolling velocity [16] and values estimated from the data obtained at a rolling speed of 1820 in/sec are $\mu_0^* = 1.01 \times 10^{-3}$ lb-sec/in$^2$, $\gamma^* = 3.77 \times 10^{-5}$ in$^2$/lb, and $\beta^* = 0.046$/deg F. In the present investigation, these values are used and all three parameters are assumed to be constant.

**Model III.** Primarily for the purpose of comparison, a constant traction coefficient is considered as a possible lubrication model. An absolute value of 0.007 is assumed for the traction coefficient. Note that the components $\kappa_1$ and $\kappa_2$ are now defined as

$$\kappa_1 = \frac{|\kappa| u_1}{|u|} \quad \text{and} \quad \kappa_2 = \frac{|\kappa| u_2}{|u|} \tag{25}$$

where $|\kappa| = 0.007$ is the absolute value of the traction coefficient.

## Dimensional Organization

If the applied force and moment vectors as computed above are substituted in equations (1) and (2), the dynamic formulation of the differential equations of motion becomes complete. With specified initial conditions, these equations may be integrated to obtain the ball motion. Before any numerical integration proce-

**Table 1 Comparison of the steady state dynamic solutions with the available quasi-static solution**

| Parameter | | Quasi-static force balance computation[a] | Traction model I | Traction model II | Traction model III |
|---|---|---|---|---|---|
| Ball angular velocity (rpm) | $\omega_{\hat{x}}$ | 57670 | 57410 | 57280 | 57950 |
| | $\omega_{\hat{y}}$ | 0 | 51 | 53 | 121 |
| | $\omega_{\hat{z}}$ | 3591 | 3990 | 4123 | 580 |
| Ball orbital velocity (rpm) | | 7255 | 7214 | 7200 | 7247 |
| Spin-to-roll-ratio | Outer race | 0 | 0.00833 | 0.0121 | 0.0823 |
| | Inner race | 0.689 | 0.679 | 0.676 | 0.754 |
| Contact angle (deg) | Outer race | 4.074 | 4.068 | 4.015 | 5.358 |
| | Inner race | 37.70 | 37.68 | 37.68 | 37.51 |
| Contact load (lb) | Outer race | 109.9 | 107.9 | 107.5 | 108.9 |
| | Inner race | 17.21 | 17.22 | 17.22 | 17.29 |

[a] Due to Jones [12].

dure is employed, the equations must, however, be nondimensionalized so that the order of truncation error at each time step may be tested and convergence of the solution is ensured. All linear dimensions have already been scaled with respect to a characteristic length $r_0$. The computed force and moment vectors, if nondimensionalized, will have scales $(p_H ab)$ and $(p_H abr_0)$, respectively, as may be easily seen from the above analysis. Thus,

$$\mathbf{F} = \frac{2\pi}{3}\sum_{i=1}^{2}\mathbf{F}_i^* p_{H_i} a_i b_i = \frac{2\pi}{3}\sum_{i=1}^{2}\mathbf{F}_i^* p_{H_i} r_0^2 A_i B_i$$

and (26)

$$\mathbf{G} = \frac{2\pi}{3}\sum_{i=1}^{2}\mathbf{G}_i^* p_{H_i} a_i b_i r_0 = \frac{2\pi}{3}\sum_{i=1}^{2}\mathbf{G}_i^* p_{H_i} r_0^3 A_i B_i$$

where $\mathbf{F}^*$ and $\mathbf{G}^*$ will represent the dimensionless force and moment vectors and the index i refers to the races.

Now since the ball position relative to the races is a function of time, the Hertzian parameters $p_H$, $a$ and $b$ will vary with time. If the static values of these parameters are $p_H{}^0$, $a^0$, and $b^0$ then clearly the static ball load $Q^0$ is

$$Q^0 = \frac{2}{3}\pi p_H{}^0 a^0 b^0 = \frac{2}{3}\pi p_H{}^0 r_0^2 A^0 B^0 \tag{27}$$

Equations (26) and (27) may now be combined to obtain

$$\mathbf{F} = Q^0\sum_{i=1}^{2} F_i^* P_i^* A_i^* B_i^*$$

and (28)

$$\mathbf{G} = Q^0 r_0 \sum_{i=1}^{2}\mathbf{G}_i^* P_i^* A_i^* B_i^*$$

The selection of outer or inner race contact for the variables $p_H{}^0$, $a^0$, and $b^0$ is arbitrary since their product at both races is equal, these parameters are determined for the outer race contact. Equation (28) may now be substituted in equations (1) and (2) to derive the time scale.

$$\tau = t\sqrt{\frac{Q^0}{mr_0}} \tag{29}$$

Assuming the ball to be spherical (moment of inertia $I = md^2/10$), the equations of motion may be written in the following dimensionless form.

$$\begin{aligned}
\frac{d^2X}{d\tau^2} &= \sum_{i=1}^{2} F_{x_i}^* P_i^* A_i^* B_i^* \\
\frac{d^2R}{d\tau^2} - (R_e + R)\frac{d^2\eta}{d\tau^2} &= \sum_{i=1}^{2} F_{r_i}^* P_i^* A_i^* B_i^* \\
(R + R_e)\frac{d^2\eta}{d\tau^2} + 2\frac{dR}{d\tau}\frac{d\eta}{d\tau} &= \sum_{i=1}^{2} F_{\eta_i}^* P_i^* A_i^* B_i^*
\end{aligned} \tag{30}$$

and

$$\begin{aligned}
\frac{d\Omega_{\hat{x}}}{d\tau} &= \frac{10}{D^2}\sum_{i=1}^{2} G_{\hat{x}}^* P_i^* A_i^* B_i^* \\
\frac{d\Omega_{\hat{z}}}{d\tau} - \Omega_{\hat{z}}\frac{d\eta}{d\tau} &= \frac{10}{D^2}\sum_{i=1}^{2} G_{\hat{y}}^* P_i^* A^* B^* \\
\frac{d\Omega_{\hat{z}}}{d\tau} + \Omega_{\hat{y}}\frac{d\eta}{d\tau} &= \frac{10}{D^2}\sum_{i=1}^{2} G_{\hat{z}}^* P_i^* A^* B^*
\end{aligned} \tag{31}$$

where

$$\begin{Bmatrix} F_x^* \\ F_r^* \\ F_\eta^* \end{Bmatrix} = \mathbf{F}^*; \quad \begin{Bmatrix} G_{\hat{x}}^* \\ G_{\hat{y}}^* \\ G_{\hat{z}}^* \end{Bmatrix} = \mathbf{G}^* \quad \text{and} \quad \begin{Bmatrix} \Omega_{\hat{x}} \\ \Omega_{\hat{y}} \\ \Omega_{\hat{z}} \end{Bmatrix} = \hat{\Omega} = \omega\sqrt{\frac{mr_0}{Q^0}}$$

By selecting the ball radius for the characteristic length, $r_0$, it is found that all variables in equations (30) and (31) are of the same order and, hence, the formulation is suitable for numerical integration. A Fourth Order Runga-Kutta-Merson method [5] is used to integrate the equations of motion. This scheme requires an additional evaluation of the derivatives at each time step to estimate the truncation error. Thus, a test on convergence of the obtained integrated solutions is possible.

## Results

A typical angular contact bearing is selected arbitrarily to ob-

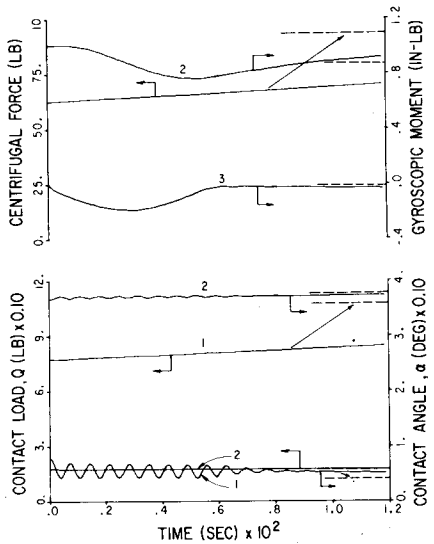


Fig. 7 Contact loads and dynamic forces and moments

tain numerical solutions of the above system of differential equations of motion. The geometry of the selected bearing is defined by the following parameters

Number of balls = 19
Outer race curvature factor = 0.52
Inner race curvature factor = 0.52
Ball diameter = 0.59375 in.
Pitch diameter = 4.13390 in.
Contact angle = 25 degrees

For obtaining steady state solutions with the above lubrication models, a thrust load of 200 lb and inner race rotation of 15000 rpm is assumed. The required time to reach a steady state will clearly depend on the selected initial conditions. The traction coefficients in the rolling directions at the center of the inner race contact in the range of such operating conditions are shown in Fig. 5 for the various traction models.

With the objective of comparing the steady state solutions with those obtained by simple force balance computations using outer race control, dynamic solutions are obtained with the above three lubrication models. The initial conditions in each case were obtained from the quasi-static outer race control solution. The results are compared in Table 1. It is seen that, since the traction coefficients in Model I and II are generally large, the two steady state solutions are fairly close to the quasi-static solution. This primarily implies that outer race control hypothesis may even hold under some EHD lubrication conditions. The main factor which determines the breakdown of this simple hypothesis is the general order of magnitude of the traction coefficient as clearly seen by the results of Model III. In this case, a relatively large gyroscope becomes possible and, hence, the ball angular velocity tends to become parallel to the bearing axis. Harris [8] has reported similar findings from his quasi-static analysis. Also, Hirano [10] has presented experimental evidence of such a behavior.

Although the results obtained with Model I and II are close to the quasi-static solution, no such general conclusion may be derived. It should be noted that the magnitude of the traction coefficient in both of the above models depend on the lubricant properties at the operating temperatures. Thus, in general for determining the ball motion precisely it may be necessary to solve the equations of motion. A significant necessity of a dynamic simulation arises when the bearing is subjected to some variations in the operating conditions. To illustrate this effect with lubrication Model II, the above bearing with 200 lb thrust load is assumed to be initially operating at 12500 rpm and the inner race speed is suddenly increased to 15000 rpm. In fact the inner race is subjected to a constant acceleration of $10^6$ rpm/sec to obtain the desired 2500 rpm increment in race speed. Such a step change in speed is perhaps an exaggeration. Nevertheless, for the dynamic solutions obtained with such conditions provide considerable insight into the transient ball motion and bearing skid.

Fig. 6 summarizes the ball motion completely in dimensionless form. The initial transient in the variables defining the center of ball are primarily due to selected initial conditions which were determined by outer race control at 12500 inner race rpm. The value of dimensionless time, $\tau$, at which the inner race reaches full speed of 15000 rpm is 2. It is clear that although the ball angular acceleration components about the $\hat{y}$ and $\hat{z}$ go to zero fairly rapidly, the $\hat{x}$ component and the orbital acceleration component assume a fairly constant value. This primarily corresponds to the flat part of the traction curve in Fig. 5 at high slip velocities. The small but gradual changes in the $X$ and $R$ coordinate of the center of the ball basically denote change in contact angle due to the increasing centrifugal force as the ball accelerates in the orbital direction. During the total time shown in Fig. 6 the ball center has moved about 7 radians, i.e., it has travelled just over one revolution. The steady increase in $\eta$ and $\omega_{\hat{x}}$ essentially determines the process of skidding in the bearing. From these rate of changes, the time required before the bearing reaches a steady state configuration may be easily estimated if the final motion is known,

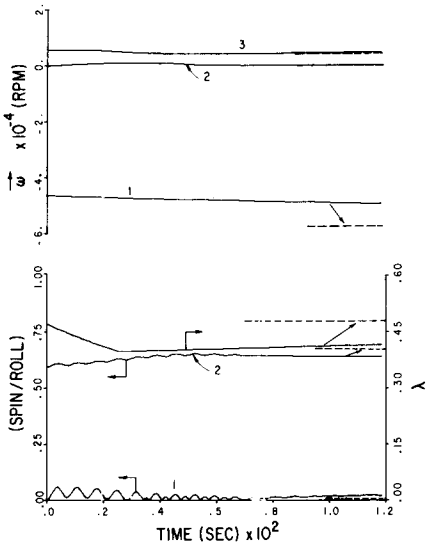


Fig. 8 Ball velocities

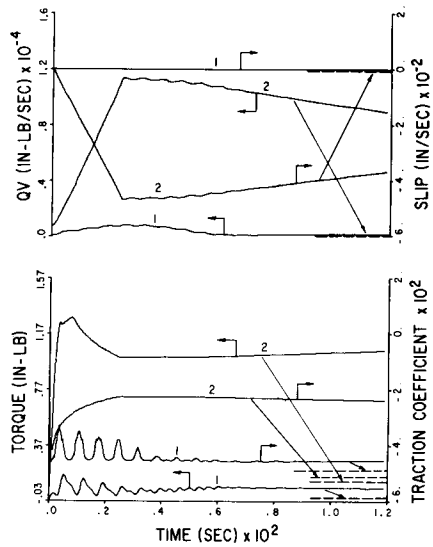


Fig. 9 Torque and slip variations of the races

which may be efficiently determined by integrating the differential equations of motion with another set of initial conditions. The steady state motion obtained in this way is shown by dashed lines in Figs. 7 to 9 when the solid curve represents the transient motion in dimensional form.

The rate of increase in contact load at the outer race due to the increasing centrifugal force is shown in Fig. 7. Also shown in this figure are the gyroscopic moments and the contact angles. As pointed out above, the initial transients in the contact angle are perhaps due to the selected initial conditions. Fig. 8 shows the angular velocity components and the spin-to-roll ratios. It is seen that the $\hat{y}$ and $\hat{z}$ components of the angular velocity vector do not change appreciably and only the $\hat{x}$ component and the orbital velocity are effected by the sudden acceleration of the inner race. The orbital velocity is represented by the parameter $\lambda$ in Fig. 8, which is defined as

$$\lambda = \frac{\text{Ball orbital velocity}}{\text{Race angular velocity}}$$

From the nondimensional results shown in Fig. 6 and the relevant time scales defined earlier it can be estimated that the

steady accelerations of the orbital and rotational motion about the $\hat{x}$ axis are approximately $3 \times 10^4$ and $4 \times 10^5$ rpm/sec, respectively. Thus the time required for reaching the steady state configuration will be approximately 0.02 to 0.04 sec. It should be noted that the acceleration does have a positive gradient with respect to time due to the nature of the traction model. In other words, for large slip rate the traction increases as the slip rate decreases.

Fig. 9 shows the slip rates and corresponding traction coefficient in the center of the contact ellipse in the direction of rolling. Also plotted in this figure are the torques about the bearing axis and a $QV$ value which is defined by the integral over the contact ellipse of the product of normal load and the absolute slip velocity. The practical significance of this parameter lies in the estimation of wear during skidding. From the classical wear theories, wear rate is primarily expressed in terms of the relation

$$W = \frac{KQV}{H} \text{ in}^3/\text{sec}$$

where $W$ = wear rate ($\text{in}^3$/sec); $K$ = wear coefficient; $Q$ = normal load (lb); $V$ = sliding velocity (in/sec) and $H$ is the hardness of the material ($\text{lb/in}^2$).

Applying the above relation incrementally over the contact ellipse the wear rate is expressed as

$$W = \frac{K}{H} \int_{-1}^{1} u(\bar{\xi})\, Q(\bar{\xi})\ d\bar{\xi}$$

where $Q\ (\xi)\ d\xi = dQ$ is the load over an infinitesimal area and the integration is performed over the entire contact ellipse.

It is the value of the above integral which is denoted as the $QV$ value in Fig. 9. Symbolically

$$QV = \int_{-1}^{1} u(\bar{\xi})\, Q(\bar{\xi})\ d\bar{\xi}$$

Thus, the results shown in Fig. 9 may be readily used to compute the expected wear due to skidding if the hardness of the material is known and the wear coefficient is approximated. The proposed analysis and the computer program developed during the present investigation thus becomes a very practical design tool for bearing selection or design against excessive wear due to skidding in applications where the races are subjected to accelerations or retardations. Also, a study of the transient solutions due to any given acceleration rate of the rotating race(s) as a function of applied thrust load will provide a relationship between wear due to skidding and the applied load. This realistic relationship will replace the simplified relation used by Poplawski and Mauriello [15] in their model for designs against skid.

## Conclusions

A dynamic analysis is presented to analyze the transient ball motion in angular contact ball bearings under realistic EHD traction conditions at the ball-race contacts. The generalized differential equations of motions are solved with prescribed initial conditions and hence the analysis is free of simplified and sometimes controversial kinematic hypotheses. It is shown that large discrepancies between the general motion and the simplified motion obtained by outer race control assumption exist when the traction coefficient is low enough to allow gyroscopic slip. In fact, the ball angular velocity vector tends to become parallel to the bearing axis under such conditions.

The generalized dynamic analysis and the computer program developed in this investigation is presented as a design tool for applications where the bearing is subjected to skid due to acceleration of the races. The formulation not only estimates the expected wear during skid but also provides a means to determine the required preload for reducing excessive skid. In summary, a complete analysis for both the steady state and transient ball motion is presented under prescribed operating conditions.

It should, however, be noted that the present analysis is free of any separator effects which may influence the ball motion. In fact it is necessary to couple the generalized ball motion presented here with the generalized equations of motion of the separator. The author hopes to include such effects and also other system dynamic factors, such as race dynamics, in the anticipated future investigations.


## Acknowledgments

The author is grateful to Dr. J. A. Walowit, Dr. A. Gu, and Mr. L. W. Winn for very helpful and enlightening discussions during this investigation.


# APPENDIX

The Hertzian contact solutions for the ball race contacts have been summarized by Harris [9]. Some of the relevant expressions are summarized here. In the case of an elliptical contact, the length of semimajor and semiminor axes of the ellipse and the contact deflection are determined by the relations

$$a = a^*\left(\frac{3Q}{2E'\Sigma\rho}\right)^{1/3}$$

$$b = b^*\left(\frac{3Q}{2E'\Sigma\rho}\right)^{1/3}$$

$$\delta = \delta^*\left(\frac{3Q}{2E'\Sigma\rho}\right)^{2/3} \cdot \frac{\Sigma\rho}{2}$$

where

$$a^* = \left(\frac{2\epsilon^2\mathcal{E}}{\pi}\right)^{1/3};\quad b^* = \left(\frac{2\mathcal{E}}{\pi\epsilon}\right)^{1/3};\quad \delta^* = \frac{2\mathcal{F}}{\pi}\left(\frac{\pi}{2\epsilon^2\mathcal{E}}\right)^{1/3};$$

$$\mathcal{E} = \int_0^{\pi/2}\left[1 - \left(1 - \frac{1}{\epsilon^2}\right)\sin^2\varphi\right]^{1/2} d\varphi;$$

$$\mathcal{F} = \int_0^{\pi/2}\left[1 - \left(1 - \frac{1}{\epsilon^2}\right)\sin^2\varphi\right]^{1/2} d\varphi$$

$\Sigma\rho = \rho_{I1} + \rho_{I2} + \rho_{II1} + \rho_{II2}$ is the sum of curvature;

$$\frac{1}{E'} = \frac{1 - \nu_I^2}{E_I} + \frac{1 - \nu_{II}^2}{E_{II}}$$ and the ratio

$\epsilon = a/b$ is determined by solving the equation

$$\frac{(\epsilon^2 + 1)\mathcal{E} - 2\mathcal{F}}{(\epsilon^2 - 1)\mathcal{E}} = \frac{(\rho_{I1} - \rho_{I2}) + (\rho_{II1} - \rho_{II2})}{\Sigma\rho}$$

The dimensionless curvature is defined by $\Sigma\rho^* = \Sigma\rho r_0$ when $r_0$ is the characteristic scaling length. All of the above equations are applied to both the inner and outer race contacts. The subscripts I and II denote race and ball and 1 and 2 denote the direction of rolling and the direction normal to rolling.

## References


1 Allen, C. W., Townsend, D. P., and Zaretsky, E. V., "Elastohydrodynamic Lubrication of a Spinning Ball in a Nonconforming Groove," JOURNAL OF LUBRICATION TECHNOLOGY, TRANS. ASME, Series F, Vol. 92. No. 1, Jan. 1970, pp. 89–96.

2 Cheng, H. S., "Calculation of Elastohydrodynamic Film Thickness in High Speed Rolling and Sliding Contacts," MTI Report No. 67TR24, 1967.

3 Cheng, H. S., "A Numerical Solution of the Elastohydrodynamic Film Thickness in an Elliptical Contact," JOURNAL OF LUBRICATION TECHNOLOGY, TRANS. ASME, Series F, Vol. 92, 1970, pp. 155–162.

4 Dawson, D., and Higginson, G. R., *Elastohydrodynamic Lubrication*, Pergamon Press, 1966.

5 Gear, C. W., *Numerical Initial Value Problems in Ordinary Differential Equations*, Prentice Hall, 1971.

6 Gu, A., "An Improved Method for Calculating the Spin Torque in Fully Lubricated Ball Race Contact," JOURNAL OF LUBRICATION TECHNOLOGY, TRANS. ASME, Series F, Vol. 95, 1973, pp. 106–108.

7 Harris, T. A., "Ball Motion in Thrust Loaded Angular Contact Bearings with Coulomb Friction," JOURNAL OF LUBRICATION TECHNOLOGY, TRANS. ASME, Series F, Vol. 93, 1971, pp. 32–38.

8 Harris, T. A., "An Analytical Method to Predict Skidding in Thrust Loaded Angular Contact Ball Bearings," JOURNAL OF LUBRICATION TECHNOLOGY, TRANS. ASME, Series F, Vol. 93, 1971, pp. 17–24.

9 Harris, T. A. *Rolling Bearing Analysis*, Wiley, 1966.

10 Hirano, F., "Motion of a Ball in Angular-Contact Ball Bearings," *ASLE Trans.*, Vol. 8, 1965, pp. 425–434.

11 Johnson, K. L., and Cameron, R., "Shear Behavior of Elastohydrodynamic Oil Film at High Rolling Contact Pressures," *Proc., I. Mech. E.*, London, Vol. 182, 1967–1968.
12 Jones A. B., "Ball Motion and Sliding Friction in Ball Bearings," *JOURNAL OF BASIC ENGINEERING*, TRANS. ASME, Mar. 1959, pp. 1–12.
13 Jones, A. B., "A General Theory for Elastically Constrained Ball and Radial Roller Bearings Under Arbitrary Load and Speed Conditions," *JOURNAL OF BASIC ENGINEERING*, TRANS. ASME, Vol. 12, No. 2, June 1960, pp. 309–320.
14 McGrew, J. M., Gu, A., Cheng, H. S., and Murray, S. F., "Elastohydrodynamic Lubrication—Preliminary Design Manual," Wright-Patterson Air Force Base Tech. Report AFAPL-TR-70-27, 1970.
15 Poplawski, J. V., and Mauriello, J. A., "Skidding in Lightly Loaded High-Speed Ball Thrust Bearings," ASME Paper No. 69-Lubs-20.
16 Smith, R. L., Walowit, J. A., and McGrew, J. M., "Elastohydrodynamic Traction Characteristics of 5P4E Polyphenyl Ether," JOURNAL OF LUBRICATION TECHNOLOGY, TRANS. ASME, Series F, Vol. 95, 1973, pp. 353–362.
17 Smith, R. L., Walowit, Gupta, P. K., and McGrew, J. M., "Research on Elastohydrodynamic Lubrication of High Speed Rolling-Sliding Contacts," Wright-Patterson Air Force Base, Tech. Report AFAPL-TR-72-56, 1972.
18 Walters, C. T., "The Dynamics of Ball Bearings," JOURNAL OF LUBRICATION TECHNOLOGY, TRANS. ASME, Series F, Vol. 93, 1971, pp. 1–10.

## DISCUSSION

### A. Gu[2]

The author is to be congratulated for presenting an important and timely paper. His ball bearing dynamics analysis accommodates any reasonable ball-race contact traction model and also provides the uniqueness of studying the transient behavior of a ball bearing when it is in acceleration or deceleration. Thus, it appears that this paper offers a useful tool for ball bearing design evaluation.

It is interesting to note that in the example given in Table 1 of the paper, EHD traction models I and II yield steady-state solutions which are quite similar to the outer-race control solution. The discussor believes that this is mainly due to the sharp rise of traction at small slip and the high level of traction in the traction curves for models I and II, as shown in Fig. 5 for the inner-race contact. In comparison with the inner-race contact, for a given gyroscopic moment there can be only very little slip in the outer-race contact because of a closer conformity. The resulting angular velocities of the ball are thus very close to those based on the outer-race control assumption. The higher the initial slope in the traction curve, the smaller the outer-race slip (the closer the solution to the outer-race control one). This is indicated by the solutions for models I and II presented in Table 1. In the limit of an infinite slope, i.e., a high constant coefficient of traction, the outer-race control solution would result. On the other hand, if the level of coefficient of traction is too low, both races would noticeably slip for the same gyroscopic moment, as indicated by the Model III solution.

As pointed out by the author, one particularly useful application of his analysis is to study the effect of preload to reduce skid during acceleration or deceleration. It would be interesting to see any of such investigations.

[2] Mechanical Technology Inc., Latham, N.Y.

With regard to future development of ball bearing dynamic analysis, the discussor fully agrees with the author that the retainer effect should be included to have a more complete simulation of ball motion. In the meantime, a more realistic and more universally valid EHD model representing the traction in a ball-race contact is needed to be incorporated in a complete ball bearing dynamics analysis.

## Author's Closure

The author is thankful to Dr. Gu for his comments. It is quite true that the slope of the traction-slip curve, in the low slip region, will in many cases dominate the validity of race control hypotheses. However, the absolute value of the traction coefficient, at any time, will also have a significant effect on the ball motion. For example, if the traction coefficient is such that the gyroscopic moment is larger than any resisting moment due to the tractive forces then the ball will slip and any ball bearing analyses and computer programs neglecting gyroscopic slip will not be relevant.

With regard to the question of preload and skid relationship, the author has carried out some preliminary work[3] to demonstrate the capability of the analysis, presented herein, in determining the optimum preload under given conditions of operation. The author expects to report some more parametric studies in this area in the near future. It is also expected that future investigations will include coupling of the ball motion analysis with generalized dynamics of the retainer. Such a comprehensive analysis will provide a real time dynamic simulation of a ball bearing under the most practical conditions of operation and hopefully deeper insight into the problems of ball and retainer instabilities will be obtained.

[3] Gupta, P. K., "Generalized Dynamic Simulation of Skid in Ball Bearings," To be Published, *AIAA Journal of Aircraft*, Vol. 12, 1975.